Available online at www.sciencedirect.com
ScienceDirect
Trans. Nonferrous Met. Soc. China 32(2022) 668−681
Transactions of Nonferrous Metals Society of China
www.tnmsc.cn

Selective depression mechanism of combination of lime and sodium humate on arsenopyrite in flotation separation of Zn–As bulk concentrate

Qian WEI, Liu-yang DONG, Cong-ren YANG, Xue-duan LIU, Fen JIAO, Wen-qing QIN

School of Mineral Processing and Bioengineering, Central South University, Changsha 410083, China

Received 16 February 2021; accepted 30 August 2021

Abstract: Lime (CaO) and sodium humate (NaHA) were used as the combined depressant for arsenopyrite pre-treated by $CuSO_4$ and butyl xanthate. Micro-flotation tests show that the combined depressant CaO and NaHA achieved the selective depression of arsenopyrite. Closed-circuit lab-scale test results indicate that the synergistic effect of CaO+NaHA achieved a satisfactory flotation separation of sphalerite and arsenopyrite, for which the Zn grade and recovery of Zn concentrate were 51.21% and 92.21%, respectively. Contact angle measurements, adsorption amount measurements and X-ray photoelectron spectroscopy analysis indicate that the dissolved calcium species (mainly as Ca^{2+}) were adsorbed on the mineral surfaces, thereby promoting NaHA adsorption. Moreover, the surface of the arsenopyrite absorbed more amount of calcium species and NaHA than that of the sphalerite, thereby accounting for the strong hydrophilic surface of arsenopyrite. The adsorption of NaHA on arsenopyrite was mainly chemical adsorption through its carboxyl groups and Ca atoms, whereas that on sphalerite surface was relatively weak.

Key words: sphalerite; arsenopyrite; Zn−As bulk concentrate; flotation separation; lime; sodium humate

1 Introduction

Arsenopyrite (FeAsS) is a most common As-bearing mineral that often closely coexists with other sulphide minerals in poly-metallic ores [1,2]. In flotation system, arsenopyrite floats along with other sulphide minerals into the concentrate and reduces its quality [3]. Any arsenic in the concentrate is harmful, because its presence will worsen the subsequent smelting process of the concentrate and causes hazards to the environment and human beings [4−7]. The removal of arsenopyrite during mineral processing is more economical than that during metallurgical processing, and the flotation separation of arsenopyrite and other sulphides is the most effective method [8−10]. Therefore, the development of high-efficient and non-toxic depressant for arsenopyrite is of great significance for improving resource utilization, subsequent smelting processes and environmental pollution reduction.

Generally, in industrial flotation plant practice, two types of ores, namely, poly-metallic sulphide ores and tin-containing poly-metallic sulphide ores, need to remove arsenopyrite [11−14]. For the beneficiation of poly-metallic sulphide ores, some depressants, including inorganic compounds (CaO, the combined $FeCl_3$+NH_4Cl, $KMnO_4$, Na_2SO_3, NaCN, $K_4[Fe(CN)_6]$ and H_2O_2) [8,15−17], and organic compounds (dextrin, NaHA, tannin and calcium lignosulfonate) [5,18,19], have been widely used and have shown excellent inhibiting effect on

Corresponding author: Wen-qing QIN, Tel: +86-731-88830884, E-mail: qinwenqing369@126.com;
Fen JIAO, Tel: +86-731-88830884, E-mail: jfen0601@126.com
DOI: 10.1016/S1003-6326(22)65824-2
1003-6326/© 2022 The Nonferrous Metals Society of China. Published by Elsevier Ltd & Science Press

arsenopyrite. Despite some reports regarding the use of the above-mentioned depressants in sequential flotation of poly-metallic sulphide ores, few attempts have been made to depress arsenopyrite in bulk concentrate of tin-containing poly-metallic sulphide ores.

A mining area of tin-containing poly-metallic sulphide ore, which is located in Inner Mongolia, China, has the cassiterite resources of 6×10^4 t (average tin grade of 1.0%). The valuable metals of the ore include tin, zinc, tungsten, to a less extent, molybdenum and bismuth. The content of harmful impurity arsenic is high, assaying 2.46%. Therefore, the control of the As content in each concentrate is the focus and difficulty of the mineral processing. To minimize the impact of sulphide minerals on the beneficiation of cassiterite, the sulphide minerals must be floated in advance. According to different floatabilities of the sulphide minerals, the principle flowsheet can be determined as "Preferential flotation of Mo/Bi—Bulk flotation of Zn/As—Flotation separation of Zn and As—Gravity of Sn/WO_3". To ensure the maximum flotation recovery, sphalerite and arsenopyrite are firstly floated with excessive dosage of $CuSO_4$ and BX in the bulk flotation stage. After pre-treatment by $CuSO_4$ and BX, the two minerals show extremely similar flotation behaviours, and their flotation separation without depressant is impossible. However, reports on the use of effective and environmentally friendly depressants for arsenopyrite in bulk Zn–As concentrate are scarce [18,20]. Moreover, the selective depression mechanism is still unclear.

In this work, according to the results of preliminary exploratory tests, the combination of CaO and NaHA expressed a good inhibiting effect on arsenopyrite and is selective for sphalerite. However, the fundamental study and their applications in the laboratory- and industrial-scale tests are limited. Therefore, this work mainly aims to investigate the selective inhibiting effect of the combined depressant CaO and NaHA on the two minerals after bulk flotation in theoretic and actual applications. Flotation experiments, contact angle measurements, adsorption amount measurements and X-ray photoelectron spectroscopy (XPS) analysis were conducted to explore the flotation behaviours of the two minerals and the possible depression mechanism.

2 Experimental

2.1 Materials

Pure samples of sphalerite and arsenopyrite used in this work were purchased from the Hunan and Yunnan Provinces, China, respectively. The lump samples were firstly crushed with a hammer to obtain small block, and then the proportion with high purity was carefully handpicked and ground in a laboratory ceramic ball mill. Secondly, the ground samples were dry sieved using the standard sieves (38 and 74 μm). The products with the particle fraction of 38−74 μm were used for micro-flotation experiments, adsorption amount measurements and XPS analysis. Samples with the particle fraction of <38 μm were further ground to below 2 μm for chemical analysis and X-ray diffraction (XRD) analysis. Chemical analysis results are shown in Table 1. According to Table 1, the sphalerite and arsenopyrite samples used in this study were of 96.34% purity and 97.13% purity, respectively. Figures 1(a) and (b) show the XRD patterns of sphalerite and arsenopyrite, respectively. As shown in Fig. 1, the two samples were of extremely high purity.

Table 1 Chemical analysis results of sphalerite and arsenopyrite (wt.%)

Sample	Zn	Fe	S	Pb	Cu	SiO_2
Sphalerite	62.34	0.57	28.51	0.36	0.04	4.26
Sample	Fe	As	S	Pb	Zn	SiO_2
Arsenopyrite	35.83	44.69	14.88	0.06	0.05	2.22

The tin-containing poly-metallic ore samples used in the laboratory-scale tests were obtained from Inner Mongolia, China. The chemical analysis results show that the samples contained 1.51% Sn, 2.64% Zn, 2.46% As, 1.89% S, 3.64% F, 0.19% WO_3, 0.02% Mo, 0.009% Bi, 0.025% Pb, 74.74% SiO_2, 6.01% Al_2O_3, 1.55% CaO, 0.98% K_2O and 0.44% Na_2O (mass fraction). The main metal minerals and the corresponding mass fractions were cassiterite (1.4%), sphalerite (3.6%), arsenopyrite (1.0%) and wolframite (0.17%). The main gangue minerals and the corresponding mass fractions were quartz and feldspar (70.1%) and mica (10.5%).

The flotation reagents used in this work were pH adjuster hydrochloric acid (HCl) and sodium

hydroxide (NaOH), activator copper sulphate ($CuSO_4$), collector sodium butyl xanthate (BX) and ethyl thiocarbamate (DDTC), frother methyl isobutyl carbinol (MIBC), depressant lime (CaO) and sodium humate (NaHA). $CuSO_4$ and NaHA were purchased from Tianjin Kemion Chemical Reagent Co., Ltd., China. MIBC and CaO were supplied by Aladdin Reagent Co., Ltd., Shanghai, China. HCl and NaOH were supplied by BSQ Chemistry Technique, Shanghai, China. They were of analytical grade with extremely high purity of ≥99%. Industrial grade BX and DDTC were received from Zhuzhou Flotation Reagent Factory in Hunan Province, China. The concentrations of HCl and NaOH were 2 and 1 mol/L, respectively. The resistivity of the distilled (DI) water (Arium Mini, Sartorius, Germany) was over 16.0 MΩ·cm.

2.2 Micro-flotation experiments

Micro-flotation experiments were carried out by a XFG flotation machine (40 mL plexiglass cell, Jinlin Exploration Machinery Plant, Changchun, China) at the agitating speed of 1602 r/min. For each test, 2.0 g of sample was firstly cleaned by ultrasonic treatment for 5 min and then dispersed into a 40 mL plexiglass cell that contained 35 mL of DI water. After stirring for 1 min, HCl or NaOH was added and stirred for 2 min. Subsequently, the flotation reagents were added into the flotation pulp in order, and each flotation reagent was added at a certain time interval. The addition order and the reaction time for each reagent are shown in Fig. 2(b). Flotation was carried out for 2 min, and the concentrate (flotation foam) was manually scraped and collected. Subsequently, the concentrate and tailing were oven-dried and weighed for recovery calculation.

For the artificial mixed minerals tests, sphalerite and arsenopyrite were manually mixed according to the mass ratio of 1:1, and then the appropriate flotation reagents were added. The reagent addition sequence and the corresponding reaction time were consistent with those of micro-flotation tests. The collected products were oven-dried, weighed and prepared for metal grade analysis, and the recovery was calculated according to the yield and metal grade.

2.3 Laboratory-scale flotation tests

Based on the properties of the raw ore mentioned in Section 2.1, the raw ore contains many valuable metals, including tin, zinc, molybdenum, bismuth and tungsten. According to the quality standard of tin concentrate, both zinc and arsenic contents in tin concentrate should be strictly controlled below 2%. Therefore, considering the subsequent recovery of cassiterite and wolframite, the sulphide minerals must be removed in advance. The flowsheet of the principle process is shown in Fig. 2(a).

A total of 1.0 kg of the sample was ground with a wet ball mill to achieve a 58% passing of 74 μm. The flotation tests were carried out using self-aerated XDF−63 flotation machine (Jilin Exploring Machinery Plant, Jilin, China). The Zn−As bulk flotation was firstly carried out to obtain Zn−As bulk concentrate from the tailing of Mo−Bi flotation process, wherein reagents $CuSO_4$, BX and MIBC were added. Next, the Zn−As bulk concentrate was separated (with 0.75 L effective volume for rougher–scavenger flotation and 0.5 L for cleaner flotation). The impeller speed was kept

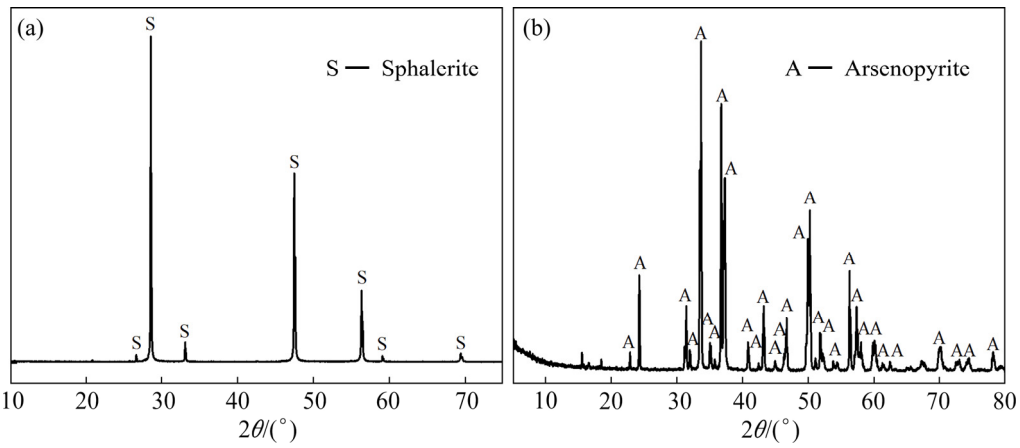

Fig. 1 XRD patterns of sphalerite (a) and arsenopyrite (b)

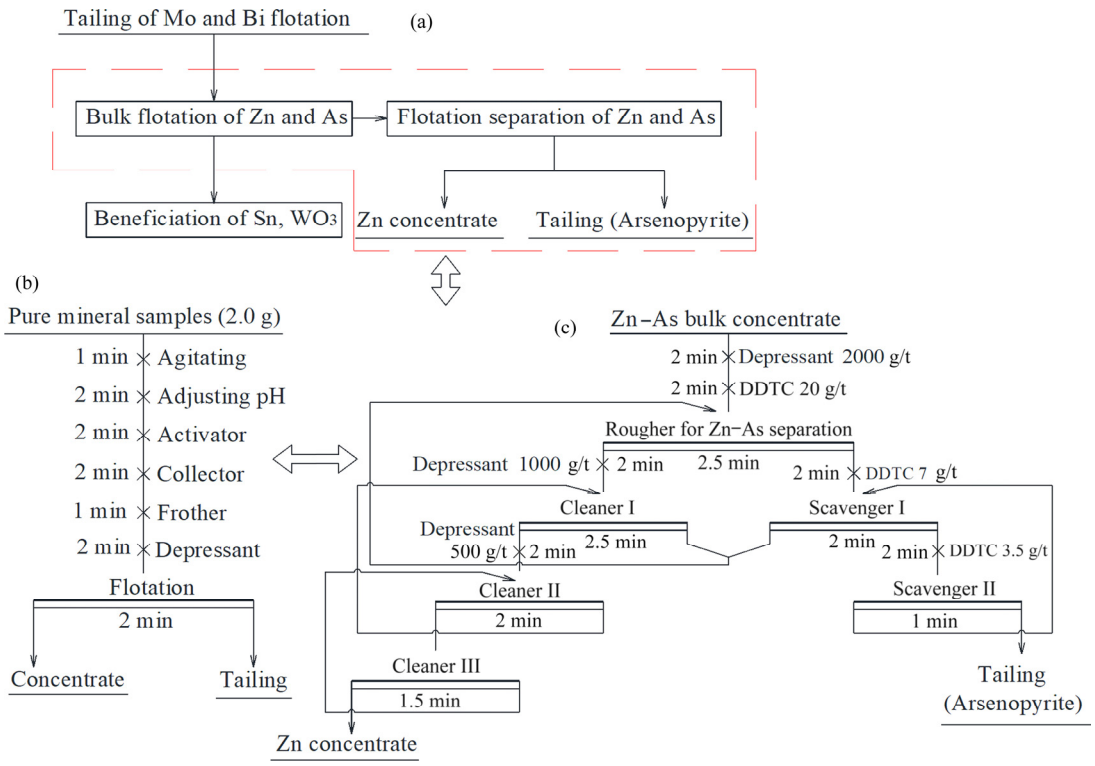

Fig. 2 Flowsheet of principle process (a), micro-flotation experiments (b) and closed-circuit lab-scale flotation tests (c)

constant at 1992 r/min. The desired flotation reagents were sequentially added into the flotation slurry at 2 min interval, and the flotation time of each operation was different and determined according to the actual flotation phenomenon. The foam product was automatically collected by a froth scarper device. Figure 2(c) presents the flowsheet of closed-circuit lab-scale flotation tests. Finally, the recovery was calculated according to the yield of the collected products and the metal grade analyzed by chemical analysis.

2.4 Contact angle measurements

The hydrophilicity and hydrophobicity of the mineral surface can be characterized by the change in the contact angle. Firstly, a lump mineral sample with a smooth surface polished by sandpapers was placed in a beaker with 35 mL DI water followed by the pH adjustment with 2 min interval. Subsequently, the sample was conditioned with the desired reagent(s), repeatedly washed with DI water and dried with N_2. The contact angle of the mineral surface was measured by a JY−82 automatic video contact angle meter (Chende Dingsheng Testing Machine Testing Equipment Co., Ltd.). The mineral sample was placed on the stage of the equipment, and then a drop of DI water was placed on the mineral surface. Thereafter, a set of microscopic images were taken, and the best view was selected and measured for the three-phase contact angle.

2.5 Adsorption amount measurements

For each adsorption amount measurement, 2.0 g of mineral sample was placed into the flotation cell with 35 mL DI water, the desired amount of flotation reagents were added into the flotation pulp, and the additive order and the conditioning time were consistent with those of micro-flotation experiments. After the interaction process, the suspensions were allowed to settle for 2 min, and then the supernatant liquid was centrifuged at 9000 r/min for 20 min. Finally, the residual concentration of calcium ions in the supernatant was measured by inductively coupled plasma optical emission spectrometry (SPECTROBLUE FMX28, ICP-OES system of Germany), and the residual amount of total organic carbon (TOC) in the supernatant was determined by a TOC-LCPH analyzer (Shimadzu, Kyoto, Japan). The amount of flotation reagents adsorbed on the mineral surface (Γ) was calculated by the difference between the initial and the residual concentrations,

as shown below:

$$\Gamma = \frac{(C_0 - C)V}{mS}$$

where V is the volume of the flotation slurry (mL); C_0 and C are the initial and residual concentrations of the flotation reagent (mg/L), respectively; m is the mass of the mineral sample (g); S is the special surface area of the mineral sample (m^2/g).

2.6 XPS analysis

The instrument of ESCALAB 250Xi (Thermo Fisher Scientific Inc, USA) with a monochromatic Al K_α-ray source at 1486.6 eV was used for XPS analysis. The narrow scanning spectra were performed using a pass energy of 20 eV and an energy scan step size of 0.1 eV, and the pressure of the analysis chamber was below 1×10^{-7} Pa. The binding energy of C 1s at 248.6 eV was used for calibration. The prepared procedure of the samples was consistent with that of micro-flotation experiments, and the treated samples were filtered, rinsed three times with DI water and oven-dried for testing. The data were collected and analyzed by Avantage 5.954 software.

3 Results and discussion

3.1 Micro-flotation results

Figure 3(a) shows the recoveries of sphalerite and arsenopyrite as a function of NaHA dosage with 5×10^{-5} mol/L $CuSO_4$ and 1×10^{-4} mol/L BX at pH 6.5. Apparently, both minerals had good floatabilities after the treatment of $CuSO_4$ and BX, and their recoveries were approximately 90%. When NaHA was added as depressant, the recoveries of both minerals remained at a high level (above 70%) with increasing NaHA dosage from 0 to 1000 mg/L. This phenomenon indicates that the flotation separation of the minerals was impossible when using NaHA as single depressant. Figure 3(b) represents the relationship between pH and the

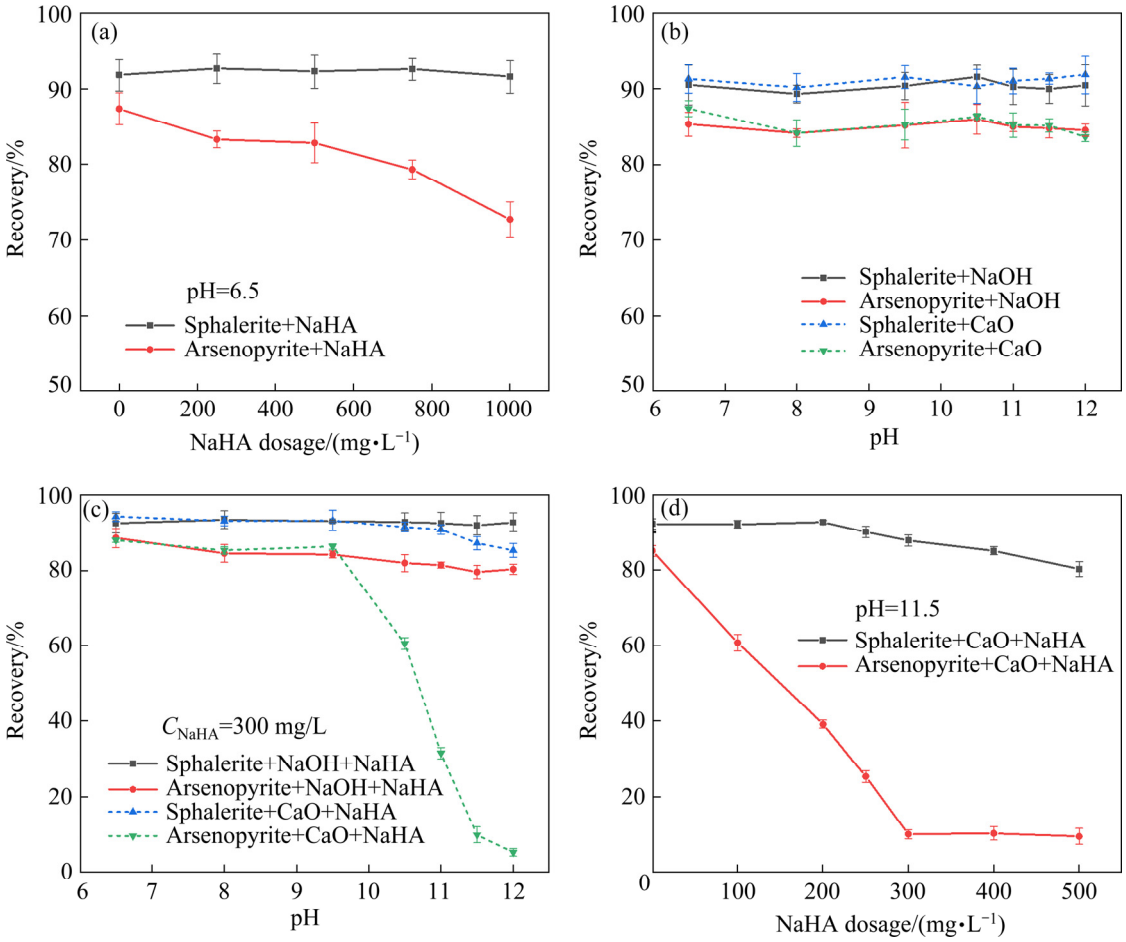

Fig. 3 Recoveries of sphalerite and arsenopyrite in the presence of 5×10^{-5} mol/L $CuSO_4$, 1×10^{-4} mol/L BX and 10 mg/L MIBC as function of NaHA dosage (a), pH value (b), pH value in the presence of NaHA (c), and NaHA dosage in the presence of CaO (d)

floatabilities of the two minerals in the presence of NaOH and CaO, respectively. In the presence of NaOH or CaO, both minerals had good floatabilities, and their recoveries were above 80% at pH 6.5−12. Apparently, separating them using NaOH or CaO as single depressant is difficult. Figure 3(c) shows the relationship between pH and the floatabilities of the two minerals in presence of the mixed depressant NaOH+NaHA and CaO+NaHA, respectively. When the mixed depressant NaOH+NaHA was added, the recoveries of both minerals were above 80% at pH 6.5−12. However, after the addition of CaO+NaHA, in the pH range of 6.5−9.5, the recovery of arsenopyrite remained at a high level. When pH was larger than 9.5, the recovery of arsenopyrite dropped significantly. The recovery of sphalerite remained constant at approximately 90% in the whole tested pH range. This result suggests that the two minerals could be separated using CaO+NaHA as the mixed depressant at pH 11−12. Figure 3(d) shows the floatabilities of the two minerals as a function of NaHA dosage in the presence of CaO at pH 11.5. As the NaHA dosage continued to increase, the recovery of sphalerite did not change greatly, but the recovery of arsenopyrite decreased significantly. When the dosage of NaHA was increased to 300 mg/L, sphalerite still had an excellent floatability of 87.87%, whilst the recovery of arsenopyrite was only 10.14%. This finding indicates that the flotation separation of the two minerals can be achieved by the addition of the combination of CaO+NaHA. These findings also indicated that the inhibiting effect of NaHA on arsenopyrite was largely promoted in the presence of calcium species dissolved by CaO.

To investigate the actual inhibiting effect of the combined depressant CaO+NaHA on arsenopyrite, artificial mixed mineral tests were carried out, and the results are shown in Fig. 4. In presence of depressant CaO+NaHA, the Zn and As grades of Zn concentrate were 59.12% and 2.05%, respectively. The large increase in the Zn grade of Zn concentrate (from 31.05% (feed) to 59.12%) suggests that the depressant CaO+NaHA had an excellent inhibiting effect on arsenopyrite. Moreover, 95.45% Zn was recovered, and only 4.62% As (the impurities) was floated into the Zn concentrate. This finding indicates that the combined depressant has minimal effect on the floatability of sphalerite. The results demonstrate that the mixed depressant CaO+NaHA can achieve satisfactory flotation separation of sphalerite and arsenopyrite.

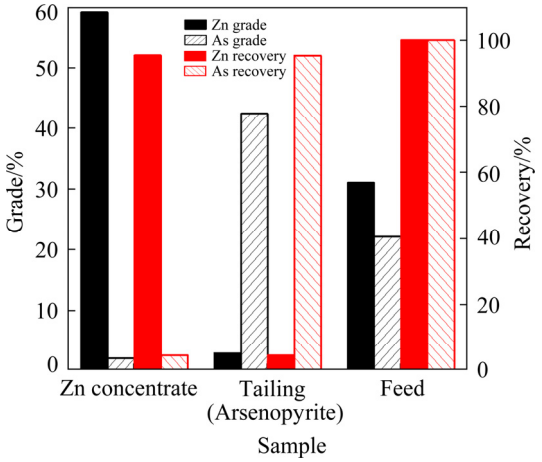

Fig. 4 Results of flotation separation of artificial mixed minerals

3.2 Laboratory-scale flotation results

Laboratory-scale flotation tests were further used to verify the inhibiting effect of the combined depressant CaO/NaHA on the flotation separation of real run-of-mine sample, and the closed-circuit flotation tests were carried out on tin-containing poly-metallic ore samples. Results of the closed-circuit flotation tests in the presence of different depressants are presented in Table 2. As shown in Table 2, when CaO (2000 g/t) or NaHA (2000 g/t) was added, the Zn grades in Zn concentrates were 32.21% and 30.53%, respectively, and the corresponding Zn recoveries were 94.34% and 92.21%, respectively. However, 75.90% and 81.63% of As metals floated and entered Zn concentrates, indicating that the flotation separation of sphalerite and arsenopyrite was not achieved using CaO or NaHA as single depressant. As expected, the addition of the combined CaO+NaHA ((1900+100) g/t) showed excellent inhibiting effect towards arsenopyrite and strong selectivity towards sphalerite. The Zn concentrate was obtained, with Zn and As grades of 51.21% and 2.15%, respectively, and the Zn recovery was 92.21%, thereby demonstrating a favourable separating results. The results also suggested that the combination of CaO+NaHA was superior to each of them alone in the flotation separation of the Zn–As bulk concentrate.

Table 2 Results of closed-circuit lab-scale flotation tests

Depressant	Dosage/ ($g \cdot t^{-1}$)	Product	Operating yield/%	Grade/%		Operating recovery/%	
				Zn	As	Zn	As
CaO	2000	Zn concentrate	83.85	32.21	22.15	94.34	75.90
		Tailing	16.15	10.04	36.52	5.66	24.10
		Zn−As bulk concentrate	100.00	28.63	24.47	100.00	100.00
NaHA	2000	Zn concentrate	86.23	30.53	23.27	92.21	81.63
		Tailing	13.77	16.15	32.78	7.79	18.37
		Zn−As bulk concentrate	100.00	28.55	24.58	100.00	100.00
CaO+NaHA	1900+100	Zn concentrate	51.10	51.21	2.15	92.21	4.47
		Tailing	48.90	4.52	48.06	7.79	95.53
		Zn−As bulk concentrate	100.00	28.38	24.60	100.00	100.00

3.3 Contact angle

The floatability of the mineral is directly characterized by the hydrophilicity and hydrophobicity of the mineral surface, which can be quantified by the changes in the three-phase contact angle. The contact angle of sphalerite under the conditioning of different flotation reagents is shown in Fig. 5. The NaHA dosage was 300 mg/L, and the pH value was fixed at 11.5. Figure 5(a) shows that the contact angle of natural sphalerite was 37.77°, thereby indicating the strong hydrophilicity of natural sphalerite surface. After the interaction with $CuSO_4$ and BX (Fig. 5(b)), the contact angle of sphalerite surface sharply increased from 37.77° to 96.50°, suggesting the formation of hydrophobic layer of dixanthogen (X_2) and cuprous xanthate (CuX) on sphalerite surface, and the significant enhancement of the floatability of sphalerite [21−24]. The contact angles were slightly declined to 88.62° and 87.17° with the addition of CaO (Fig. 5(c)) and NaHA (Fig. 5(d)) as single depressant, respectively, implying that the addition of CaO or NaHA had minimal effect on the hydrophobicity of the sphalerite surface. From Fig. 5(e), in the presence of the combination of CaO+NaHA, the slight decrease in contact angle (from 96.50° to 80.92°) was observed, indicating that the hydrophobicity of sphalerite surface did not change greatly. This finding suggested that the depressant CaO+NaHA had minimal effect on the contact angle of sphalerite. Moreover, under this condition, sphalerite still exhibited good floatability.

The contact angles of arsenopyrite with and without treatment with different flotation reagents are shown in Fig. 6. As shown in Fig. 6(a), the contact angle of arsenopyrite was 64.34°, suggesting that natural arsenopyrite surface had a certain degree of hydrophilicity. After the treatment with $CuSO_4$ and BX (Fig. 6(b)), the hydrophobicity of the arsenopyrite surface was largely improved, and the contact angle increased to 92.44°, indicating the formation hydrophobic layer of dixanthogen (X_2) and cuprous xanthate (CuX) on the arsenopyrite surface; thus, the floatability of arsenopyrite was dramatically increased [23]. After the addition of CaO (Fig. 6(c)) or NaHA (Fig. 6(d)) as single depressant, the contact angles of arsenopyrite slightly decreased to 82.11° and 82.46°, respectively, implying that the hydrophobicity and floatability of arsenopyrite were still good. However, the addition of the combined depressant CaO+NaHA greatly decreased the contact angle to 48.15°, suggesting that the combined CaO+NaHA had a strong inhibiting effect on arsenopyrite. Therefore, the floatability of arsenopyrite in the presence of the combined CaO+NaHA was poor. The above results were in good agreement with those of flotation tests, in which the combined depressant CaO+NaHA selectively reduced the floatability of arsenopyrite but not sphalerite.

3.4 Adsorption amount

From the above results, the inhibiting effect of NaHA on arsenopyrite can be largely promoted in the presence of the dissolved calcium species. The addition of CaO introduced large number of calcium-containing species into the flotation system, and according to the calcium species distribution

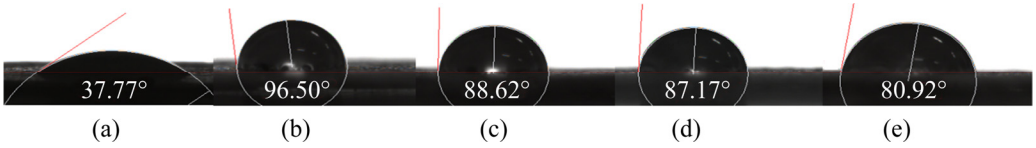

Fig. 5 Contact angles of sphalerite (a), sphalerite+$CuSO_4$+BX (b), sphalerite+$CuSO_4$+BX+CaO (c), sphalerite+$CuSO_4$+BX+NaHA (d), and sphalerite+$CuSO_4$+BX+CaO+NaHA (e)

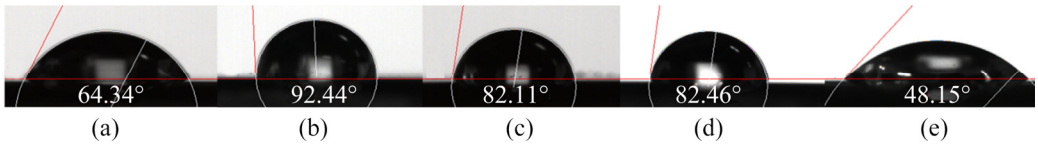

Fig. 6 Contact angles of arsenopyrite (a), arsenopyrite+$CuSO_4$+BX (b), arsenopyrite+$CuSO_4$+BX+CaO (c), arsenopyrite+$CuSO_4$+BX+NaHA (d), and arsenopyrite+$CuSO_4$+BX+CaO+NaHA (e)

diagram as a function of pH, Ca^{2+} existed as the most dominant calcium species in aqueous solution in pH range of 6−12 [24−26]. To quantitatively analyze the amounts of Ca^{2+} and NaHA adsorbed on the two mineral surfaces, $CaCl_2$ was used to simulate CaO and introduce calcium-species in slurry. The results of adsorption amount measurements are shown in Fig. 7. As shown in Fig. 7(a), the adsorption amount of Ca^{2+} increased with increasing the $CaCl_2$ dosage on both mineral surfaces. However, the adsorption amount of Ca^{2+} on arsenopyrite surface was obviously much higher than that of sphalerite within the whole tested dosage of 10−150 mg/L, suggesting that the Ca^{2+} adsorption was selective. From Fig. 7(b), in the absence of $CaCl_2$, the adsorption amount of NaHA on both mineral surfaces gradually increased with the NaHA dosage, and the maximum adsorption amounts of NaHA on sphalerite and arsenopyrite surfaces were 2.67 and 3.29 mg/m^2, respectively. However, in the presence of $CaCl_2$, the maximum adsorption amount of NaHA on sphalerite surface slightly increased to 6.03 mg/m^2, whereas that on arsenopyrite surface dramatically increased to 15.85 mg/m^2. This finding indicates that the addition of Ca^{2+} promotes the adsorption of NaHA on both mineral surfaces, but the NaHA adsorption amount on arsenopyrite surface is much higher. These results further highlight the synergistic effect between calcium-species and NaHA, and indicate much great affinity of NaHA towards arsenopyrite compared with sphalerite in the absence and presence of CaO. Therefore, the synergistic effect of CaO and NaHA provides a good selective separation of sphalerite and arsenopyrite, which is consistent with flotation tests and contact angle measurements.

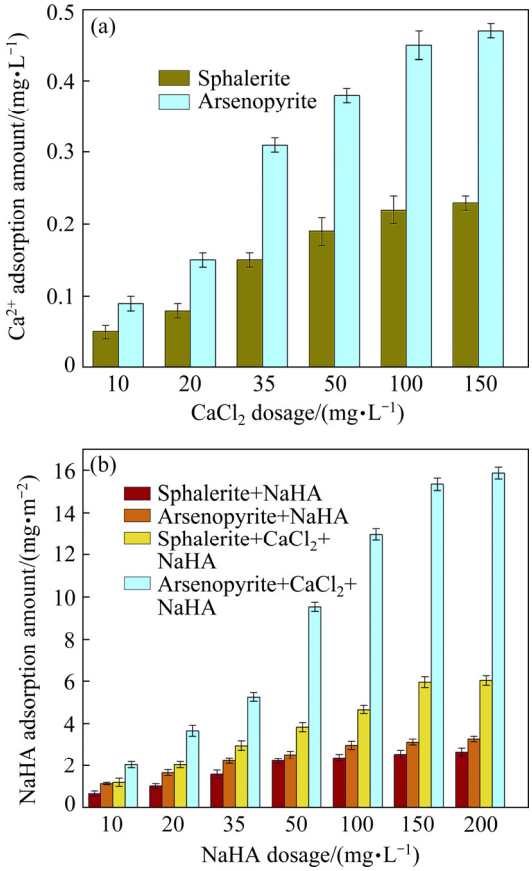

Fig. 7 Adsorption amount of Ca^{2+} on mineral surfaces as function of $CaCl_2$ dosage (a) and adsorption amount of NaHA as function of NaHA dosage in the absence and presence of 150 mg/L $CaCl_2$ (b)

3.5 XPS spectra

To further understand the deeper inhibiting

mechanism between the combined depressant and the two minerals, XPS analysis was used to investigate the type and molar fraction of the surface species on the mineral surfaces [27,28]. Table 3 depicts the molar fractions and their shifts (*D*-value) of the surface elements of the two minerals before and after treatment with flotation reagents. Table 4 shows the binding energies and

Table 3 Molar fractions and shifts (*D*-value) of surface elements of two minerals before and after treatment with flotation reagents

Item	Molar fraction/%							
	C 1s	O 1s	S 2p	Cu 2p	Ca 2p	N 1s	Fe 2p	As 3d
1# Aspy+Cu^{2+}+BX	30.69	33.40	10.00	1.57	−	−	10.60	13.74
2# Aspy +Cu^{2+}+BX+CaO	31.83	30.56	10.59	2.11	1.14	−	10.60	13.16
3# Aspy+Cu^{2+}+BX+NaHA	33.39	31.87	9.81	1.36	−	0.81	9.93	12.83
4# Aspy+Cu^{2+}+BX+CaO+NaHA	43.51	28.61	8.13	2.09	1.03	0.85	6.22	9.57
D-value (3# and 1#)	2.70	−1.53	−0.19	−0.21	−	0.81	−0.67	−0.91
D-value (4# and 2#)	11.68	−1.95	−2.46	−0.02	−0.11	0.85	−4.38	−3.59

Item	Molar fraction/%						
	C 1s	O 1s	S 2p	Cu 2p	Ca 2p	N 1s	Zn 2p
5# Sp+Cu^{2+}+BX	23.31	9.35	36.50	9.81	−	−	21.04
6# Sp+Cu^{2+}+BX+CaO	24.92	12.10	32.92	9.98	0.12	−	19.96
7# Sp+Cu^{2+}+BX+NaHA	26.64	7.41	35.35	10.63	−	0.63	19.35
8# Sp+Cu^{2+}+BX+CaO+ NaHA	32.01	10.66	31.09	9.66	0.35	1.05	15.18
D-value (7# and 5#)	3.33	−1.94	−1.15	0.82	−	0.63	−1.69
D-value (8# and 6#)	7.09	−1.44	−1.83	−0.32	0.23	1.05	−4.78

Aspy: Arsenopyrite; Sp: Sphalerite

Table 4 Binding energies and chemical shifts (*D*) of surface elements of two minerals before and after treatment with flotation reagents

Item	Binding energy/eV							
	C 1s	O 1s	S 2p	Cu 2p	Ca 2p	N 1s	Fe 2p	As 3d
1# Aspy+Cu^{2+}+BX	248.8	531.10	162.46	932.31	−	−	707.32	41.57
2# Aspy+Cu^{2+}+BX+CaO	248.8	530.99	162.36	932.31	347.35	−	707.24	41.43
3# Aspy+Cu^{2+}+BX+NaHA	248.8	531.26	162.59	932.42	−	399.79	707.48	41.63
4# Aspy+Cu^{2+}+BX+CaO+NaHA	248.8	531.10	162.46	932.36	347.47	399.86	707.26	41.49
D-value (3# and 1#)	−	0.16	0.13	0.11	−	−	0.16	0.06
D-value (4# and 2#)	−	0.11	0.10	0.05	0.12	−	0.02	0.06

Item	Binding energy/eV						
	C 1s	O 1s	S 2p	Cu 2p	Ca 2p	N 1s	Zn 2p
5# Sp+Cu^{2+}+BX	248.8	532.51	161.60	932.49	−	−	1021.64
6# Sp+Cu^{2+}+BX+CaO	248.8	532.43	161.69	932.40	348.57	−	1021.59
7# Sp+Cu^{2+}+BX+ NaHA	248.8	532.38	161.63	932.51	−	404.88	1021.62
8# Sp+Cu^{2+}+BX+CaO+NaHA	248.8	532.13	161.70	932.48	347.95	404.87	1021.61
D-value (7# and 5#)	−	−0.13	0.03	0.02	−	−	−0.02
D-value (8# and 6#)	−	−0.30	0.01	0.08	−0.62	−	0.02

the chemical shifts (*D*-value) of the surface elements of the two minerals before and after treatment with flotation reagents. For sphalerite treated with NaHA alone, as shown in Table 3 (*D*-value for 7# and 5#), the molar fraction of C 1s on sphalerite was only increased by 3.33%. From Table 4 (*D*-value for 7# and 5#), minimal changes in the binding energies of S 2p, Cu 2p and Zn 2p were observed (0.03, 0.02 and −0.02 eV, respectively), and those were within the scanning step of 0.1 eV. This finding indicated that the depressant NaHA was weakly adsorbed on sphalerite surface. After the addition of the combined depressant CaO+NaHA, the C content increased by 7.09% (Table 3, *D*-value for 8# and 6#). Thus, the increment value of C content originated from the carbon chain of NaHA after the addition of CaO was 3.76%, and the binding energy of Ca 2p shifted by −0.62 eV (Table 4, *D*-value for 8# and 6#). This result suggested that the presence of CaO promoted the adsorption of NaHA on sphalerite surface, and NaHA might mainly interact with sphalerite surface through Ca atoms.

After the treatment by depressant NaHA, according to Table 3 (*D*-value for 3# and 1#), for arsenopyrite, the C content only increased by 2.70%. Moreover, the addition of single NaHA shifted the binding energies of S 2p, Cu 2p, Fe 2p and As 3d by 0.13, 0.11, 0.16 and 0.06 eV, respectively, as shown in Table 4 (*D*-value for 3# and 1#), suggesting that NaHA was chemically adsorbed on arsenopyrite surface. The addition of CaO+NaHA increased the C content on arsenopyrite by 11.68% (Table 3, *D*-value for 4# and 2#). Therefore, the increment value of C content originated from the carbon chain of NaHA after the addition of CaO was 8.98%, and the shifts of the binding energies of S 2p and Ca 2p were 0.10 and 0.12 eV (Table 4, *D*-value for 4# and 2#), respectively. The results indicate that CaO also promotes the adsorption of depressant NaHA on arsenopyrite surface, and NaHA might mainly interact with arsenopyrite surface through S and Ca atoms.

The high-resolution spectra and peak fitting of C 1s of the two minerals were presented to reveal the specific changes in the chemical environment of the mineral surfaces with and without the addition of different flotation reagents, as shown in Figs. 8−10. From the comparison of Figs. 8(a), 9(a) and 10(a), for sphalerite, the chemical state of the C element did not change much before and after the addition of the depressants. In Fig. 8(a), for original sphalerite (pre-treated by $CuSO_4$ and BX), after peak was separated and fitted, three characteristic peaks appeared at 284.80, 286.39 and 288.63 eV, which were attributed to C—C/C—H, C—O and S—C═S, respectively [11,29,30]. Regardless of the absence (Fig. 9(a)) or the presence of CaO (Fig. 10(a)), after the treatment of NaHA, three characteristic peaks appeared at the positions with similar binding energies, and no new peaks were observed. The results indicate that NaHA is weakly adsorbed on sphalerite surface in the absence and presence of CaO.

For original arsenopyrite (pre-treated by $CuSO_4$ and BX), from Fig. 8(b), after peak was separated and fitted, Peak 1 (284.80 eV), Peak 2 (286.47 eV) and Peak 3 (288.63 eV) were observed and could be assigned to C—C/C—H, C—O and S—C═S, respectively [11,29,30]. In Fig. 9(b), the chemical state of C element did not change much after the addition of NaHA as single depressant,

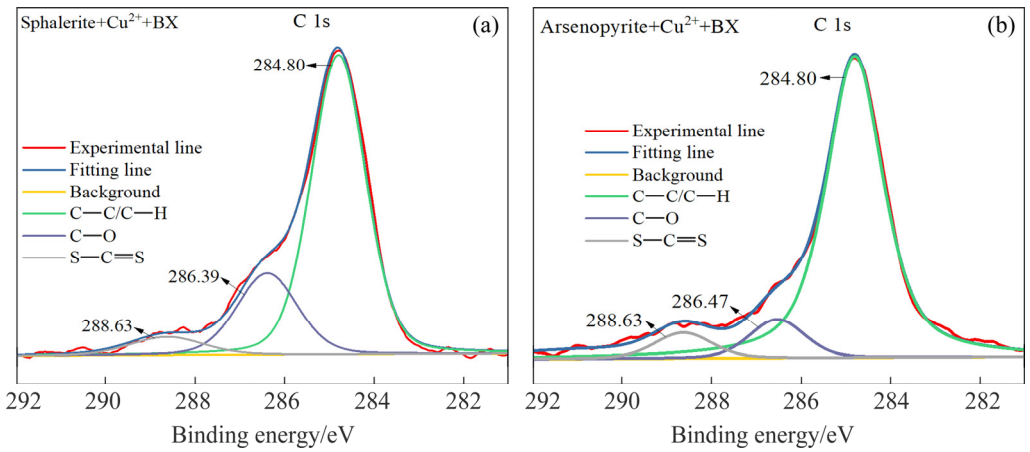

Fig. 8 Fitting peaks of C 1s of sphalerite (a) and arsenopyrite (b)

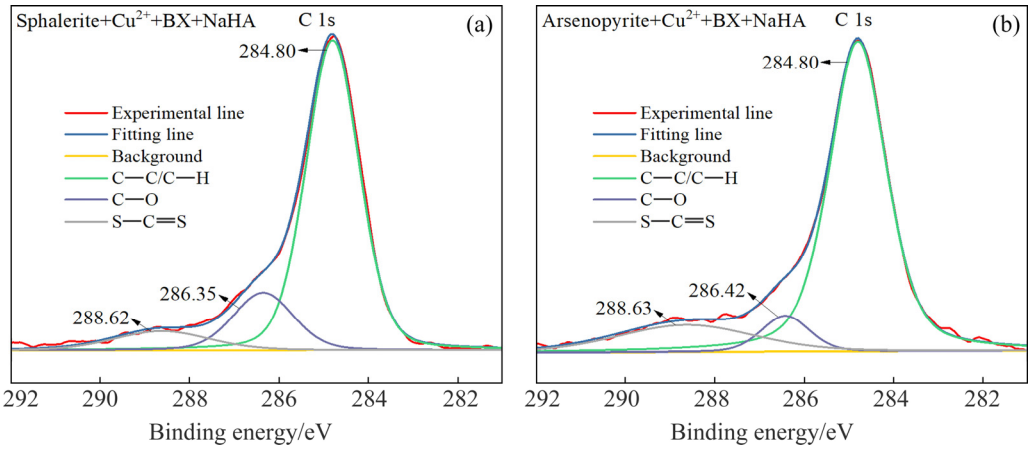

Fig. 9 Fitting peaks of C 1s of sphalerite (a) and arsenopyrite (b) in the presence of NaHA

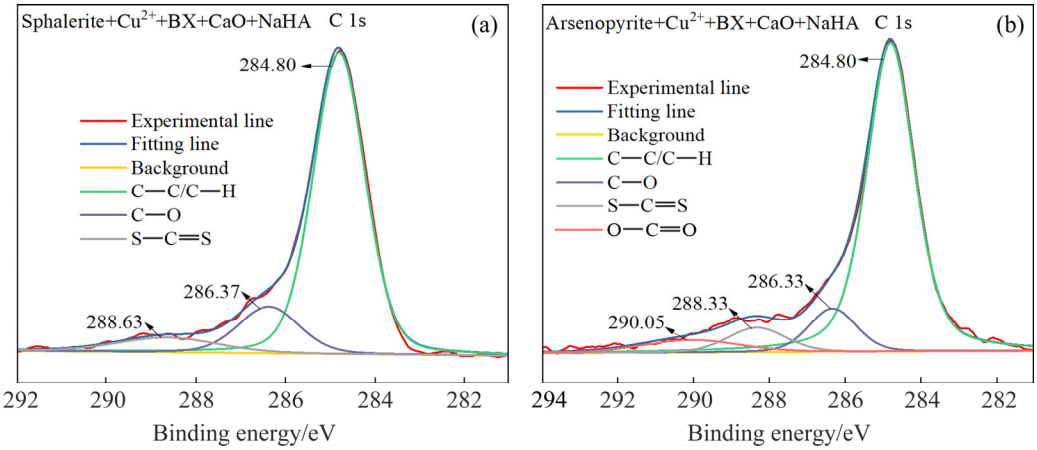

Fig. 10 Fitting peaks of C 1s of sphalerite (a) and arsenopyrite (b) in the presence of combination of CaO+NaHA

three peaks were also found at the similar positions at 284.80 (C—C/C—H), 286.42 (C—O) and 288.63 eV (S—C═S) [11,29,30], respectively, suggesting that single NaHA had a weak effect on arsenopyrite surface. However, when the combined depressant CaO+NaHA was added, in addition to the above three similar fitting peaks appeared, after the separation and fitting of the peak, a new fitting peak at 290.05 eV (O—C═O) was observed. As we all know, the carboxyl groups in NaHA structure gave it a strong ability of complexation with heavy metals [31−33]. Therefore, the new fitting peak may be attributed to the chemical interaction between the carboxyl groups (—COOH) in the molecular structure of NaHA and Ca atoms on arsenopyrite surface. The results further verify that the adsorption of NaHA on arsenopyrite surface is enhanced and promoted by the addition of CaO. Under this condition, the depressant NaHA had much stronger adsorption on the surface of arsenopyrite than that on the surface of sphalerite. This finding was in good agreement with those of flotation experiments, adsorption amount and contact angle measurements.

4 Adsorption model

Many carboxylic and phenolic groups exist in the molecular structure of NaHA. In the flotation system, NaHA has a hydrophilic character, the capability of complexation with heavy metals and mineral surface adsorption [34]. Therefore, NaHA can be used as depressant in the field of mineral processing to promote separation of different minerals. Results of flotation tests showed that a combined inhibiting effect of CaO+NaHA was more effective than that of individual and combined depressant NaOH+NaHA. Moreover, the combined depressant CaO+NaHA had a much great inhibiting effect on arsenopyrite compared with that on sphalerite at pH 11−12. All the surface measurements, including contact angle and

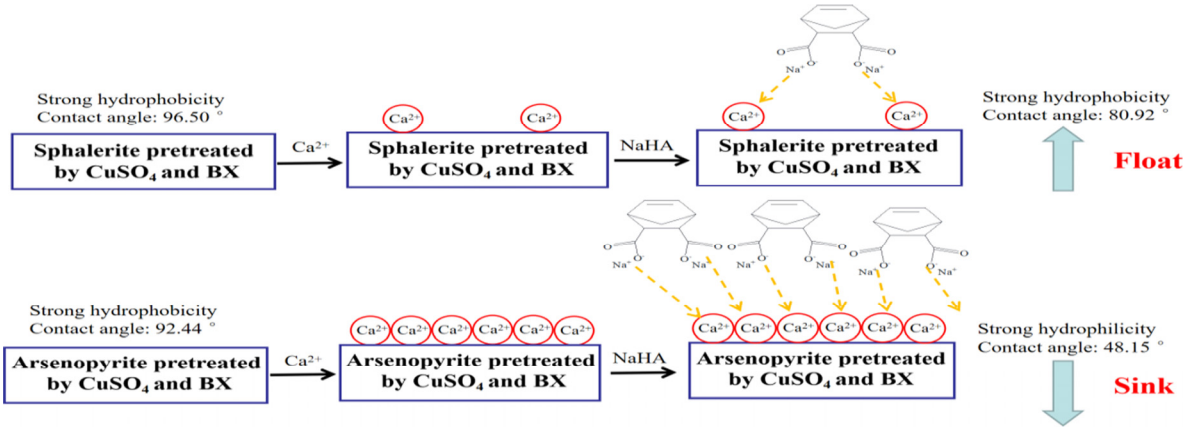

Fig. 11 Schematic diagram on mechanism of flotation separation of sphalerite and arsenopyrite

adsorption amount measurements, and XPS analysis, indicated that the combined CaO+NaHA depressant was selectively adsorbed on arsenopyrite surface and thus selectively enhanced the hydrophilicity of arsenopyrite. The dissolved calcium species (mainly as Ca^{2+}) were considerably adsorbed on the arsenopyrite surface, which promoted NaHA adsorption. According to the results in the measurements, the schematic diagram on the mechanism of the flotation separation of sphalerite and arsenopyrite is proposed and shown in Fig. 11.

5 Conclusions

(1) Micro-flotation results showed that when the NaHA dosage was 300 mg/L, sphalerite still had an excellent floatability of 87.87%, whilst the recovery of arsenopyrite was only 10.14% at pH 11.5. Results of artificial mixed minerals indicated that the Zn grade of Zn concentrate was largely increased compared with the feed ore (from 31.05% to 59.12%) using CaO+NaHA as the combined depressant, and the Zn recovery was 95.45%. Laboratory-scale tests further verified that the combined CaO/NaHA could act better than each of them alone, good indexes of flotation separation with a Zn grade of 51.21% and a Zn recovery of 92.21% were obtained at the CaO+NaHA dosage of (1900+100) g/t.

(2) Adsorption amount measurements showed that the surface of arsenopyrite adsorbed more amount of Ca^{2+} and NaHA than that of the sphalerite, and the pre-deposited Ca-species on arsenopyrite surface largely promoted NaHA adsorption, thereby resulting in the strong hydrophilicity of its surface, as demonstrated by the results of the contact angle tests.

(3) XPS analysis further verified that the dissolved Ca species were considerably adsorbed on the arsenopyrite surface, which promoted NaHA adsorption. It also provided the evidence that the chemical adsorption of NaHA mainly occurred through its carboxyl groups and the Ca atoms on arsenopyrite surface.

Acknowledgments

This work was financially supported by the National Natural Science Foundation of China (Nos. 51974364, 51904339, 52074355), and the 13th Five-Year National Key R&D Program of China (No. 2020YFC1909203)

References

[1] KYZAS G Z, MATIS K A. Methods of arsenic wastes recycling: Focus on flotation [J]. Journal of Molecular Liquids, 2016, 214: 37−45.

[2] YU Li, LIU Quan-jun, LI Shi-mei, DENG Jiu-shuai, LUO Bin, LAI Hao. Adsorption performance of copper ions on arsenopyrite surfaces and implications for flotation [J]. Applied Surface Science, 2019, 488: 185−193.

[3] VALDIVIESO A L, SÁNCHEZ LÓPEZ A A, ESCAMILLA C O, FUERSTENAU M C. Flotation and depression control of arsenopyrite through pH and pulp redox potential using xanthate as the collector [J]. International Journal of Mineral Processing, 2006, 81: 27−34.

[4] YU Li, LIU Quan-jun, LI Shi-mei, DENG Jiu-shuai, LUO Bin, LAI Hao. Depression mechanism involving Fe^{3+} during arsenopyrite flotation [J]. Separation and Purification and

Technology, 2019, 222: 109−116.

[5] LIU Rui-zeng, LI Jia-lei, WANG Yun-wei, LIU Dian-wen. Flotation separation of pyrite from arsenopyrite using sodium carbonate and sodium humate as depressants [J]. Colloids and Surfaces A, 2020, 595: 124669.

[6] LU Ji-wei, TONG Zhong-yun, YUAN Zhi-tao, LI Li-xia, Investigation on flotation separation of chalcopyrite from arsenopyrite with a novel collector: N-butoxycarbonyl-O-isobutyl thiocarbamate [J]. Minerals Engineering, 2019, 137: 118−123.

[7] RAN Jin-cheng, QIU Xian-yang, HU Zhen, LIU Quan-jun, SONG Bao-xu, YAO Yan-qing. Enhance flotation separation of arsenopyrite and pyrite by low-temperature oxygen plasma surface modification [J]. Applied Surface Science, 2019, 480: 1136−1146.

[8] LONG G, PENG Y J, BRADSHAW D. Flotation separation of copper sulphides from arsenic minerals at Rosebery copper concentrator [J]. Minerals Engineering, 2014, 66−68: 207−214.

[9] PARK K, CHOI J, GOMEZ-FLORES A, KIM H. Flotation behavior of arsenopyrite and pyrite, and their selective separation [J]. Materials Transactions, 2015, 56: 435−440.

[10] HE Ming-fei, QIN Wen-qing, LI Wei-zhong, ZHENG Ke. Pyrite depression in marmatite flotation by sodium glycerine−xanthate [J]. Transactions of Nonferrous Metals Society of China, 2011, 21: 1161−1165.

[11] WEI Qian, DONG Liu-yang, JIAO Fen, QIN Wen-qing, PAN Zu-chao, CUI Yan-fang. The synergistic depression of lime and sodium humate on the flotation separation of sphalerite from pyrite [J]. Minerals Engineering, 2021, 163: 106779.

[12] ANGADI S I, SREENIVAS T, JEON H S, BAEK S H, MISHRA B K. A review of cassiterite beneficiation fundamentals and plant practices [J]. Minerals Engineering, 2015, 70: 178−200.

[13] LEISTNER T, EMBRECHTS M, LEIβNER T, CHELGANI S C, OSBAHR I, MÖCKEL R, PEUKER U A, RUDOLPH M. A study of the reprocessing of fine and ultrafine cassiterite from gravity tailing residues by using various flotation techniques [J]. Minerals Engineering, 2016, 96/97: 94−98.

[14] LI Yu-qiong, LONG Qiu-rong, CHEN Jian-hua. Molecular structures and activity of organic depressants for marmatite, jamesonite and pyrite flotation [J]. Transactions of Nonferrous Metals Society of China, 2010, 20: 1993−1999.

[15] DONG Jing-shen, LIU Quan-jun, YU Li, SUBHONQULOV S H. The interaction mechanism of Fe^{3+} and NH_4^+ on chalcopyrite surface and its response to flotation separation of chalcopyrite from arsenopyrite [J]. Separation and Purification Technology, 2021, 256: 117778.

[16] SILVA J C M, dos SANTOS E C D, de OLIVEIRA A D, HEINE T, de ABREU H A D, DUARTE H A. Adsorption of water, sulfates and chloride on arsenopyrite surface [J]. Applied Surface Science, 2018, 434: 389−399.

[17] DONG Zai-zheng, ZHU Yi-ming, HAN Yue-xin, GAO Peng, GU Xiao-tian, SUN Yong-sheng. Chemical oxidation of arsenopyrite using a novel oxidant—Chlorine dioxide [J]. Minerals Engineering, 2019, 139: 105863.

[18] TAPLEY B, YAN D. The selective flotation of arsenopyrite from pyrite [J]. Minerals Engineering, 2003, 16: 1217−1220.

[19] SIRKECI A A. Electrokinetic properties of pyrite, arsenopyrite and quartz in the absence and presence of cationic collectors and their flotation behaviours [J]. Minerals Engineering, 2000, 13: 1037−1048.

[20] ZANIN M, LAMBERT H, du PLESSIS C A D. Lime use and functionality in sulphide mineral flotation: A review [J]. Minerals Engineering, 2019, 143: 105922.

[21] EJTEMAEI M, NGUYEN A V. Characterisation of sphalerite and pyrite surfaces activated by copper sulphate [J]. Minerals Engineering, 2017, 100: 223−232.

[22] EJTEMAEI M, NGUYEN A V. A comparative study of the attachment of air bubbles onto sphalerite and pyrite surfaces activated by copper sulphate [J]. Minerals Engineering, 2017, 109: 14−20.

[23] WANG Jing-yi, LIU Qing-xia, ZENG Hong-bo. Understanding copper activation and xanthate adsorption on sphalerite by time-of-flight secondary ion mass spectrometry, X-ray photoelectron spectroscopy, and in situ scanning electrochemical microscopy [J]. The Journal of Physical Chemistry C, 2013, 117(39): 20089−20097.

[24] KHOSO S A, LYU Fei, MENG Xiang-song, HU Yue-hua, SUN Wei. Selective separation of chalcopyrite and pyrite with a novel and non-hazardous depressant reagent scheme [J]. Chemical Engineering Science, 2019, 209: 115204.

[25] FU Ya-feng, ZHU Zhang-lei, YAO Jin, HAN Hui-li, YIN Wan-zhong, YANG Bin. Improved depression of talc in chalcopyrite flotation using a novel depressant combination of calcium ions and sodium lignosulfonate [J]. Colloids and Surfaces A, 2018, 558: 88−94.

[26] KHOSO S A, HU Yue-hua, LÜ Fei, GAO Ya, LIU Run-qing, SUN Wei. Xanthate interaction and flotation separation of H_2O_2-treated chalcopyrite and pyrite [J]. Transactions of Nonferrous Metals Society of China, 2019, 29: 2604−2614.

[27] DONG Liu-yang, WEI Qian, QIN Wen-qing, JIAO Fen. Selective adsorption of sodium polyacrylate on calcite surface: Implications for flotation separation of apatite from calcite [J]. Separation and Purification Technology, 2020, 241: 116415.

[28] PAN Zu-chao, WANG Yun-fan, WEI Qian, CHEN Xin-tao, JIAO Fen, QIN Wen-qing. Effect of sodium pyrophosphate on the flotation separation of calcite from apatite [J]. Separation and Purification Technology, 2020, 242: 116408.

[29] FREDRIKSSON A, HOLMGREN A. An in situ ATR-FTIR study of the adsorption kinetics of xanthate on germanium [J]. Colloids and Surfaces A, 2007, 302: 96−101.

[30] LIU Jian, WANG Yu, LUO De-qiang, CHEN Lu-zheng, DENG Jiu-shuai. Comparative study on the copper activation and xanthate adsorption on sphalerite and marmatite surfaces [J]. Applied Surface Science, 2018, 439: 263−271.

[31] CHEN Chen, HU Yue-hua, ZHU Hai-ling, SUN Wei, QIN Wen-qing, LIU Run-qing, GAO Zhi-yong. Inhibition performance and adsorption of polycarboxylic acids in calcite flotation [J]. Minerals Engineering, 2019, 133: 60−68.

[32] DONG Liu-yang, WEI Qian, JIAO Fen, QIN Wen-qing. Utilization of polyepoxysuccinic acid as the green selective depressant for the clean flotation of phosphate ores [J].

Journal of Cleaner Production, 2021, 282: 124532.
[33] WANG Dao-wei, JIAO Fen, QIN Wen-qing, WANG Xing-jie. Effect of surface oxidation on the flotation separation of chalcopyrite and galena using sodium humate as depressant [J]. Separation Science and Technology, 2018, 53: 961−972.
[34] LIU Run-zeng, QIN Wen-qing, JIAO Fen, WANG Xing-jie, YANG Yong-jun, LAI Chun-hua. Flotation separation of chalcopyrite from galena by sodium humate and ammonium persulfate [J]. Transactions of Nonferrous Metals Society of China, 2016, 26: 265−271.

组合抑制剂石灰和腐植酸钠在锌砷混合精矿浮选分离中对毒砂的选择性抑制机理

魏 茜，董留洋，杨聪仁，刘学端，焦 芬，覃文庆

中南大学 资源加工与生物工程学院，长沙 410083

摘 要：采用石灰和腐植酸钠作为经硫酸铜活化和丁黄药捕收后毒砂的组合抑制剂。纯矿物浮选试验表明，组合抑制剂石灰和腐植酸钠能选择性地抑制毒砂。实验室小型闭路试验结果表明，石灰和腐植酸钠的协同抑制作用能较好地实现闪锌矿和毒砂的浮选分离，得到锌精矿中锌品位为 51.21%、锌回收率为 92.21%的良好指标。通过接触角测试、吸附量测试和 X 射线光电子能谱研究组合抑制剂的抑制机理。机理研究表明，溶解钙组分(主要为钙离子)吸附于矿物表面，促进腐植酸钠的吸附；毒砂表面比闪锌矿表面吸附更多的钙组分和腐植酸钠，使毒砂表面具有强亲水性。腐植酸钠在毒砂表面的化学吸附主要是通过其分子结构中的羧基与毒砂表面的钙原子发生作用，而其在闪锌矿表面的吸附较弱。

关键词：闪锌矿；毒砂；锌砷混合精矿；浮选分离；石灰；腐植酸钠

(Edited by Wei-ping CHEN)